

Z. RANACHOWSKI^{1*}, P. RANACHOWSKI¹, A. BRODECKI¹, M. KOPEĆ¹, S. KUDELA JR²**QUASI-STATIC AND DYNAMIC TESTING OF CARBON FIBER REINFORCED MAGNESIUM COMPOSITES**

Two types of composites, consisting of pure magnesium matrix reinforced with two commercially used carbon fibers, were systematically studied in this paper. The composites fabricated by the pressure infiltration method, were subjected to quasistatic and dynamic compression tests. Morphology of fiber strands was observed using scanning electron microscope (SEM). The application of carbon fibre reinforcement led to the stiffening of tested materials, resulting in the limitation of the possible compression to approx. 2.5%. The performed tests revealed the remarkable difference in compression strength of investigated compositions. The cause of that effect was that GRANOC fiber reinforced composite exhibited insufficient bond quality between the brittle fibers and the ductile matrix. T300 reinforced composite presented good connection between reinforcement and matrix resulting in increased mechanical properties. Investigated composites demonstrated higher mechanical strength during deformation at high strain rates. Microscopic observations also proved that the latter fibers with regular shape and dense packaging within the filaments are proper reinforcement when designing the lightweight composite material.

Keywords: Mg matrix composite, compressive properties, carbon fiber, Split-Hopkinson Pressure Bar

1. Introduction

Magnesium and its alloys are promising materials for fabrication of high strength and lightweight composites [1]. Magnesium matrix composites reinforced with carbon fiber exhibit higher specific strength and stiffness in comparison to metallic materials and magnesium itself. Magnesium and carbon show clearly different physical properties and chemical nature. From the point of view of the interconnection between these elements, the different chemical nature can be important. Magnesium is alkaline earth metal (IIA group) – fairly reactive element of low electronegativity (1.31 in Pauling scale) and of low ionization energy. It has generally electropositive character. Carbon (IV group) represents considerably higher electronegativity (2.55 in Pauling scale) and creates as a rule strong covalent bonds with different degree of polarity. Taking into account the different chemical nature and potential electrostatic bonds, a good connection between magnesium matrix and carbon fibres can be expected. However, corrosive processes and microcells forming could appear in the presence of moisture, as is the case of corroding of aluminium in presence of graphite. It should be added that bonding between magnesium and carbon in composites has generally not adhesive but reactive nature. Moreover, magne-

sium – fairly reactive metal – tends to passivate. As a result of this effect the presence of magnesium oxide on the interface is standard for this type of composites.

The limitations of technical application of pure magnesium and its alloys are related to their low elastic modulus and ductility, poor creep and abrasion resistance. These limitations can be overridden by the introduction of one of the following methods:

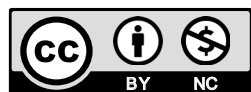
- (1) precipitation hardening,
- (2) grain size strengthening,
- (3) solid solution strengthening (alloying).

The role of precipitations and the comparison of mechanical properties of some Mg-Li-Al and Mg-Li-Zn alloys were discussed in [2]. Ultra-fine-grained Mg alloys and composites were objects of investigation in [3] and [4]. Selection of the proportions of amount of Al and Li additions in the alloying process to improve the corrosion resistance and formability of the resulted alloy were presented in [5]. The ultimate tensile stress (UTS) determined in pure magnesium can be estimated in the range of 120-160 MPa. Magnesium alloys (excluding those fabricated applying rapid solidification process) exhibit improved UTS in range of 200-300 MPa. Increased demands of application as aerospace and defense technologies encouraged the efforts to introduce the additional reinforcements to the

¹ INSTITUTE OF FUNDAMENTAL TECHNOLOGICAL RESEARCH POLISH ACADEMY OF SCIENCES, 5B PAWIŃSKIEGO STR., 02-106 WARSZAWA, POLAND

² INSTITUTE OF MATERIALS AND MACHINE MECHANICS SLOVAK ACADEMY OF SCIENCES, 9 DUBRAVSKA CESTA, 845-13 BRATISLAVA, SLOVAK REPUBLIC

* Corresponding author: zranach@ippt.pan.pl



lightweight matrix structures. Dynamic response and constitutive behavior of Mg based nanocomposites in wide temperature range was described in [6]. Deformation and fracture of Saffil fiber (SF) reinforced Mg and MgLi matrix composites was monitored in-situ by means of scanning electron microscopy during 3-point bend tests in [7]. In this paper it was pointed out that poor interfacial bond causes premature failure of the SF/Mg composite. Improved interfaces in SF/Mg12Li composite resulted in multiple cross-breakage of aligned fibers which was indicative of their participation in the composite strengthening. However in [8] the adverse process of the chemical reaction with the SF fibers imposed by the aggressive components of the Mg-Li – matrix was reported. In [9] the mechanical properties of the magnesium matrix composites reinforced with high Young modulus carbon fibres were presented. The structure of the fibre-matrix interface was analyzed using different microscopic techniques. The relevant conclusion stated in the paper was that magnesium matrix exhibit good wetting to the carbon fibres and that this matrix did not significantly react chemically with carbon. In [10] the authors tested the process of fabricating Mg and Mg-Al alloy composite reinforced with 0.27-0.74 vol.% of commercial multi-walled carbon nanotubes by using powder metallurgy techniques. UTS of specimens prepared by applying the above mentioned techniques reached 340 MPa what is still below the parameters to achieve by typical Al alloys.

With the increasing demands from industry for high strength and light-weight materials, magnesium composites reinforced with carbon fibers becoming a promising solution [11-12]. An example of the innovative application of metal-carbon composite is described in the patented device developed under support of the Leonardo Aviation Company [13]. The device, intended as tubular casing for weapons included the metal-carbon reinforcement elements. The other potential applications of these materials are automotive and aircraft industries as well as a variety of prosthetic facilities. Lightweight composites could replace the commercially used aluminum or magnesium alloys. It should be also mentioned that the carbon fibers and magnesium are not particularly expensive materials therefore they could be an alternative to traditional materials [14-16]. Despite the number of papers related to mechanical properties of magnesium/carbon fiber composites [17-23], the dynamic response of these materials was not investigated. Therefore, in present paper, comparison of static and dynamic response of two composites fabricated applying pure magnesium matrix unidirectionally reinforced by commercially available

carbon fibres is shown. Presented results extend the knowledge of mechanical behavior of Mg/C composites presented in [9].

2. Materials and methods

2.1. Composites preparation

The composite materials were fabricated by using the pressure infiltration method. The inter-fiber spaces were evacuated and subsequently filled with liquid metal (pure magnesium) at temperature of 750°C using an inert gas (Argon) with the pressure of 4 MPa for 60 s. Both composites were characterized by equal carbon fiber volume content (45%). Two types of carbon fibers were used in this study: GRANOC fibers with highly ordered internal structure [10] and T300 fibers with less ordered internal structure in comparison to GRANOC [24]. Nippon Graphite Fiber Corporation fabricates carbon fibers of GRANOC type by high temperature carbonization process applied to a pitch precursor. Pitch is a viscoelastic material composed of aromatic hydrocarbons such as: asphalt, coal tar or plant resin. T300 fibers are fabricated by carbonization process of organic polyacrylonitrile (PAN) polymer. PAN based commercial T300 carbon fiber was introduced by the Toray Company of Japan in 1971. More information on mechanical properties and fabrication techniques of both materials can be found in [26].

The detailed information about properties of used carbon fibers was presented in Table 1.

TABLE 1

Data on carbon fibers T300 and GRANOC

Carbon fiber	Fiber type	Young's modulus [GPa]	Tensile strength [GPa]	Density [$\text{g}\cdot\text{cm}^{-3}$]	Diameter [μm]
Torayca T300 (Toray)	PAN	230	3.53	1.76	7
GRANOC (Nippon Graphite)	PITCH	860	3.50	2.20	10

Composite structures were fabricated in the form of cylindrical billets with 12 mm of diameter and 10 mm length. As prepared composite samples were then wire-cut parallel to the fiber strands in order to obtain a sample with specific dimension

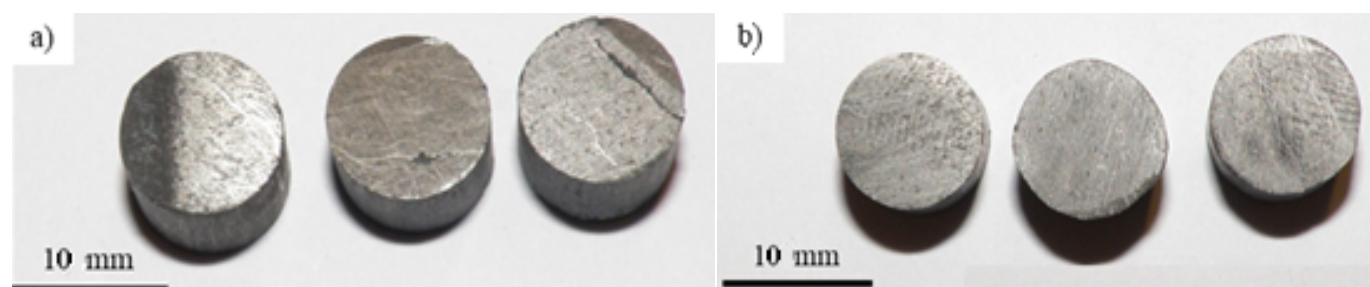


Fig. 1. Set of the composite specimens of type G (Mg + GRANOC) (a) and of type T (Mg + T300) (b) prepared for mechanical test

of 10 mm in diameter and 10 mm in height. Figure 1 presents the set of specimens prepared for mechanical tests. However one minor crack is visible at one specimen of G type and the other one at the one specimen of T type they were of not significant influence to the results of the further mechanical tests. All tests were performed at room temperature.

2.2. Composite structure

Morphology of fiber strands consisting the preforms was observed using JEOL JSM6460 LV scanning electron microscope (SEM) and presented in Figures 2-3. The fibers presented in these Figures were situated at the broken surfaces of the additional specimens left after the procedure of the fabrication of the composites. GRANOC fibers were characterized by irregular packing structure as well as the coarse fiber surface as shown in Figure 2a and Figure 2b respectively.

In contrast, T300 fibers were characterized by regular packing structure and smooth surface as shown in Figure 3a and Figure 3b respectively. The micrographs reveal that the packing of the T300 fibers was more dense than those of GRANOC type.

Before the mechanical testing, the microstructural analysis of composite cross sections was performed. As presented in Figure 4b, GRANOC fibers were characterized by irregular shape of its strands. Some number of cracks and voids in the matrix in proximity of the fibers are visible in Figure 4b. T300 fibers were characterized by regular structure as shown in Figure 4a. The remarkable lower amount of voids can be noticed near the edges of T300 fibers. These fibers were also more resistant to internal crack forming while machining. The more regular packing of T300 fibers than GRANOC fibers and more uniform micro-composition of that first composite is visible in Figures 2-4 and also in Figure 10.

2.3 Quasi-static and dynamic compression tests

Quasi-static compression tests were performed by using hydraulic MTS-858 testing machine of 250 kN capacity. The displacement velocity of the operating traverse during the tests was 0.2 mm/min. The dynamic, high strain rate compression tests were performed by using Split-Hopkinson Pressure Bar (SHPB) device installed in the Institute of Fundamental Technological Research, Warsaw. The details of the procedure applied in the

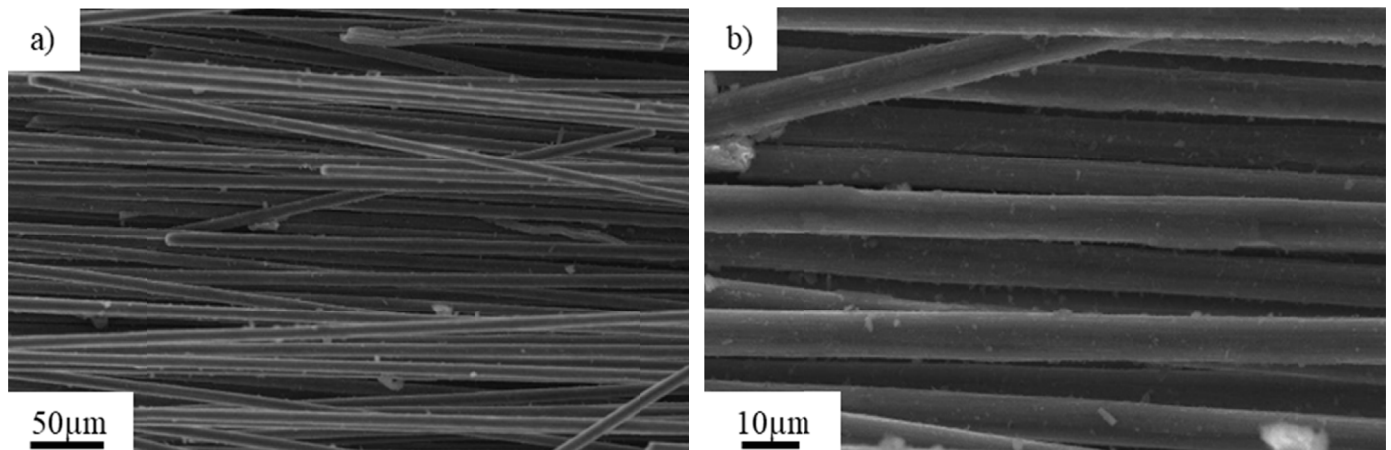


Fig. 2. SEM micrographs of the GRANOC fibers. Magnification $\times 300$ (a) and $\times 1000$ (b)

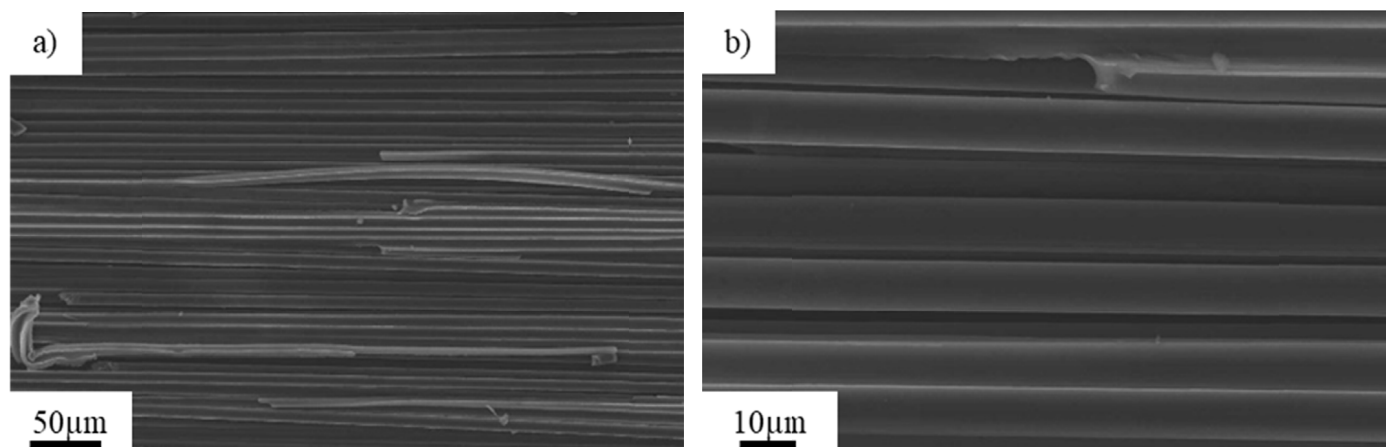


Fig. 3. SEM micrographs of the T300 fibers. Magnification $\times 300$ (a) and $\times 1000$ (b)

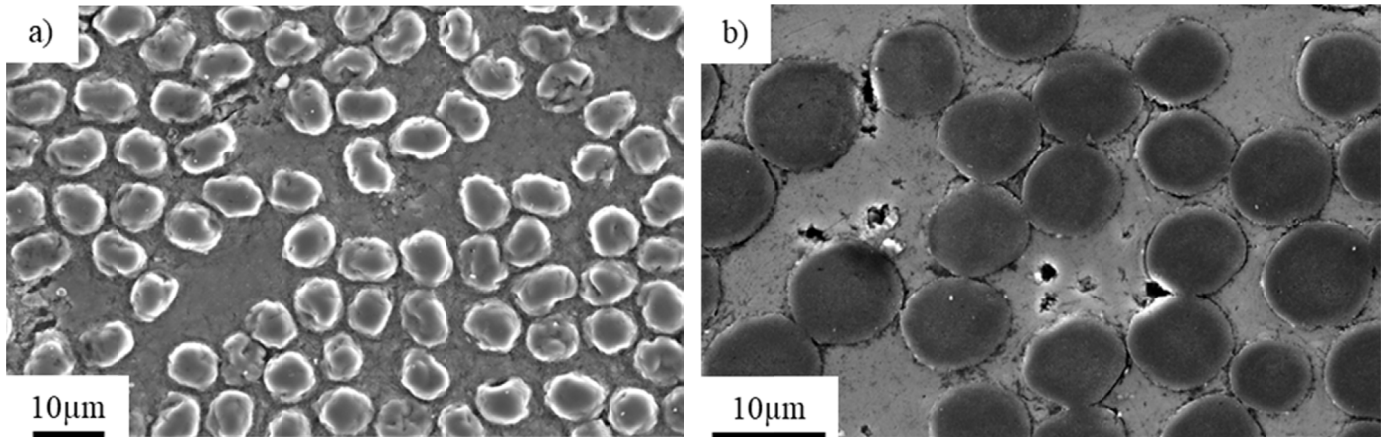


Fig. 4. SEM microstructure of the fibers' cross sections – Mg + T300 (a) and Mg + GRANOC (b) composites



Fig. 5. View of the of the Split-Hopkinson Pressure Bar device used in the research. Projectile launching device including the pressurized gas chamber is visible at far left

paper and related to testing of magnesium based nanocomposites in wide range of temperatures were described in [25]. The device used in present research was able to generate a well – controlled and repeatable loading pulses so that the specimens undertook

the compression at a rate of $10^3/s \pm 15\%$. The view of applied SHPB device is presented in Figure 5 and its schematic diagram in Figure 6.

The cylindrical specimens have been tested using SHPB device consisting of two circular aluminum bars (incident and transmitted bar) with a diameter of 20 mm, and a length of 1050 mm and 1080 mm, respectively. A stress wave was generated by launching of a 135 grams projectile with a velocity of 20 m/s toward the incident bar. Projectile velocity was experimentally determined in order to deform the composite specimens with strain rate of $10^3/s$. Upon reaching the specimen, the incident wave was split into two components. One of which, the transmitted wave, travelled through the specimen and the transmitted bar, causing the compression of the specimen. The other wave, called the reflected wave, was reflected from the specimen and travelled back down the incident bar. Two sets of four strain gauges installed at both bars were applied to measure strain. The signals evoked in the strain gauges were amplified in a two channel 60 Decibels wideband amplifier and then stored in two channel Tektronix DPO 3014 digital oscilloscope applying a sampling frequency of 25 Mega samples per second. Assuming that the deformation within the specimen is uniform, the stress / strain characteristics and deformation velocity could be

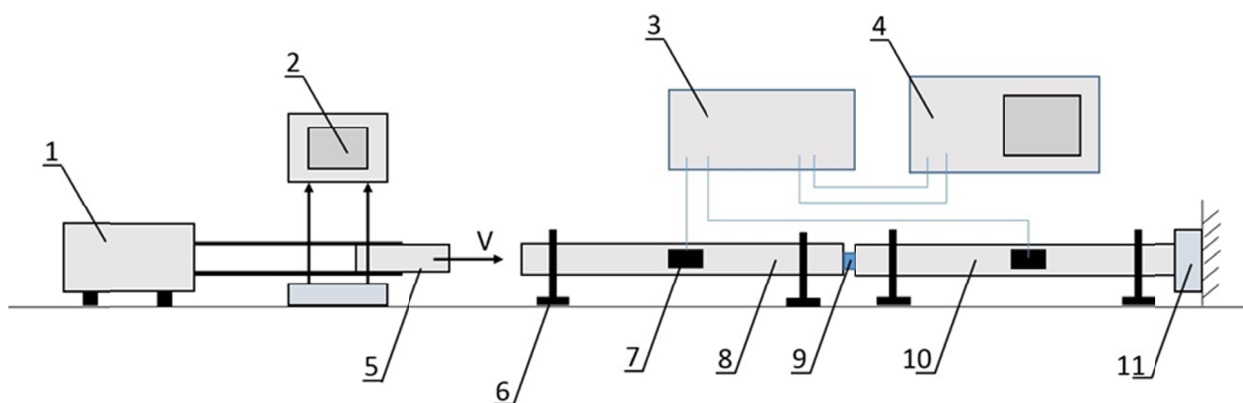


Fig. 6. Schematic diagram of Split-Hopkinson Pressure Bar device: 1 – projectile launching device with barrel to accelerate the projectile; 2 – opto-electronic system for measuring the projectile speed; 3 – wideband amplifier to process the signals from the strain gauges; 4 – two channel digital storage oscilloscope; 5 – projectile; 6 – bearing of bar system; 7 – strain gauge; 8 – incident bar; 9 – specimen; 10 – transmitted bar; 11 – damper of the elastic wave

calculated from the amplitudes of the transmitted and reflected waves [13]:

$$\sigma(t) = E_0 \frac{A_0}{A} \varepsilon_T(t) \tag{1}$$

$$\varepsilon(t) = -\frac{2C_0}{L} \int_0^t \varepsilon_R(t) dt \tag{2}$$

$$\dot{\varepsilon}(t) = \frac{2C_0}{L} \varepsilon_R(t) \tag{3}$$

where: E_0 is the Young’s modulus of the bars (70 GPa), A_0 is the cross section of the bars, A and L are specimen cross section and length respectively, ε_T and ε_R are transmitted and reflected wave amplitudes measured by the strain gauges, $\dot{\varepsilon}$ is deformation speed, C_0 is the bar longitudinal wave velocity (estimated as 6300 m/s).

3. Results and discussion

Fabricated composites were subjected to static and dynamic loading and stress-strain curves were obtained as shown in Figures 7-8. The structure of composite specimens after mechanical testing are shown in Figure 9. The important result of the mechanical tests was that the crack system was observed in the matrix material volume, which one was of significant lower strength than the fiber reinforcement. The microstructural observations were performed by using SEM technique and are further presented in Figure 10.

Static and dynamic response of G type (Mg + GRANOC) composite are shown in Figure 7. The application of carbon fiber reinforcement of very high Young’s modulus (860 GPa) has caused stiffening of the material so that the possible compression was limited to approx. 2.5%. Larger deformation caused the fracture of the sample as presented in Figure 9. No significant difference in term of stress was observed by comparing the quasi-static and dynamic test. One can find that composite subjected to both static and dynamic loading underwent brittle decomposition. It was concluded that such low strength properties correspond to the poor connection between relatively brittle carbon fibers and magnesium matrix. Such poor connection may

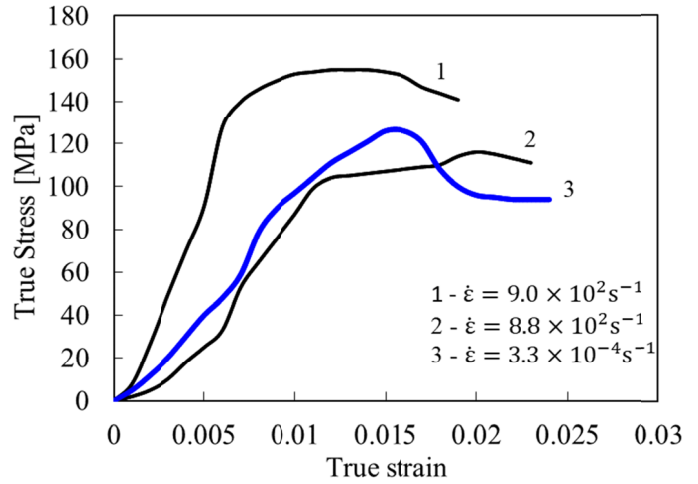


Fig. 7. Results of the mechanical testing of G type composite. Black curves represents the dynamic test results and blue curve – results the quasi-static test

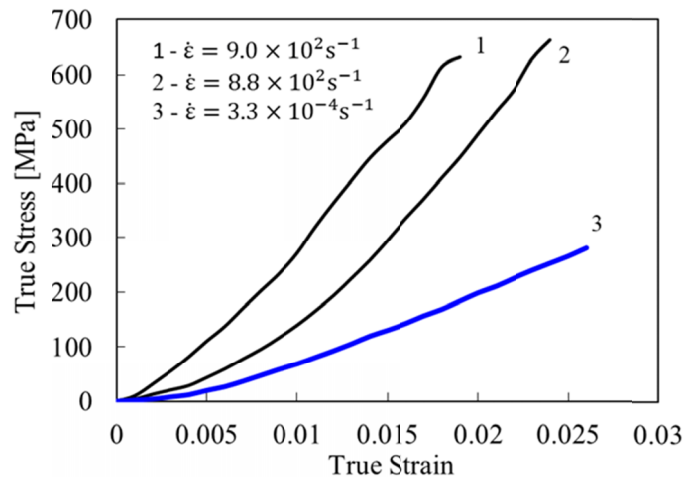


Fig. 8. Results of the mechanical tests of T type composites. Black curves represents the dynamic test results and blue curve results of the quasi-static test

cause the occurrence of micro voids and other discontinuities within material structure and subsequently lead to deterioration of mechanical properties.

The results of mechanical testing of T type (Mg + T300) composite are presented in Figure 8. The application of carbon

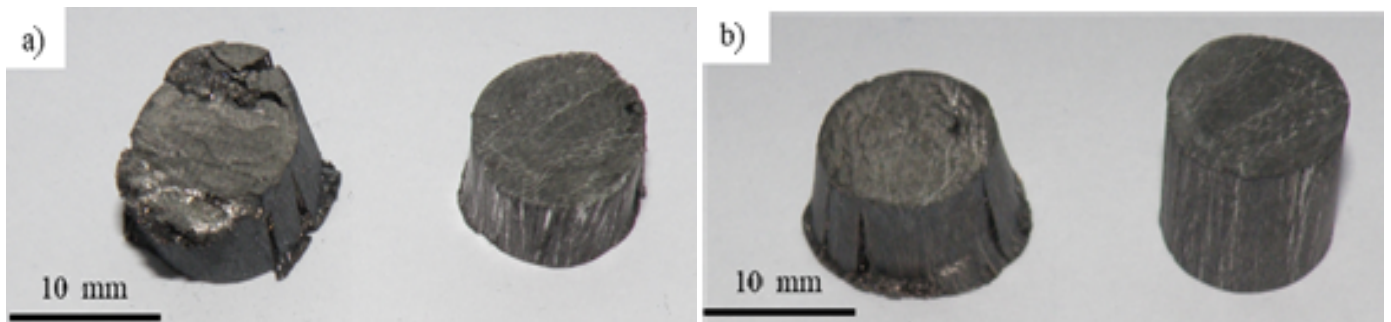


Fig. 9. View of the composite specimens after dynamic (left) and static (right) and deformation tests: type G (Mg + GRANOC) (a) and type T (Mg + T300) (b)

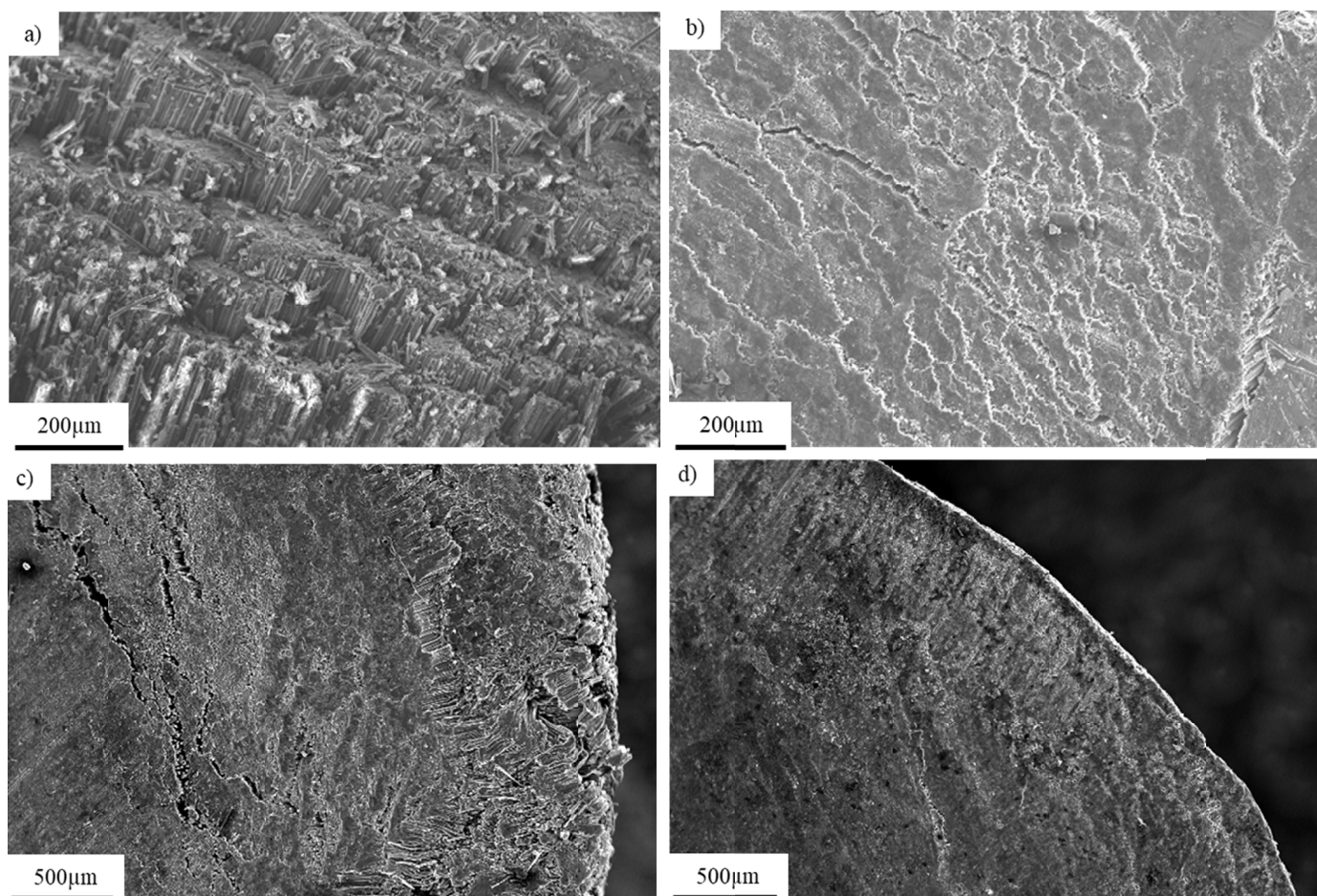


Fig. 10. The microstructural observations of fabricated composites: Mg + GRANOC after static tension test (a), Mg + T300 after static tension test (b), Mg + GRANOC after dynamic tension test (c), Mg + T300 after dynamic tension test (d)

fiber reinforcement in this type of composite has caused the remarkable stiffening of the material. In comparison to type G composite, the significant increase of strength was observed. During dynamic tests, compressive strength of 600 MPa was achieved without creation of visible cracks on the material surface as shown in Figure 9b. Smooth characteristics of the stress-strain curves presented in Figure 8 denotes the absence of early crack growth processes inside of loaded T type composite. The relatively low value of Young's modulus (230 GPa) and regular packing structure of T300 strands have resulted in high overall performance of the composite.

In order to explain the fracture mechanisms during mechanical testing, SEM technique was used to study fracture surfaces of composites. The surfaces of specimens of both composite types, deformed after the performed tests, are presented in Figure 10. The structure of Mg + GRANOC composite after both, static and dynamic tests, was depressurized, demonstrating many voids between the matrix and the reinforcement. This was probably the effect of insufficient bond between the brittle fibers and the ductile matrix. It was observed in that propagation of crack during dynamic deformation of GRANOC reinforced composite started from the edge of the sample. Several perpendicular strands of cracks were also observed in the middle part of specimen (Fig. 10c). The structure of composite reinforced

with T300 fibers was characterized by some cracks observed on the specimens surface as presented in Figure 10b. Despite the occurrence of these cracks, composite material held out both static and the dynamic loading. The bond between the matrix and the reinforcement was good and no depressurization effects were noticed. T300 reinforced composite exhibited very good connection between reinforcement and matrix resulting not only in increased mechanical properties, but also in absence of crack propagation usually initiated from the edge of the sample (Fig. 10d). Registered high mechanical strength of T300 composite was also caused by its uniform and dense microstructure. Crack formation and propagation were successfully arrested in this composite.

4. Conclusions

Presented test results of magnesium/carbon fiber composite specimens had proved that high compressive strength under dynamic loading is possible to achieve under condition of the application of the proper reinforcement.

The use of Split-Hopkinson Bar testing method enabled for determination of behavior of investigated material in presence of dynamic impacts being a typical hazard in practical application conditions. Smooth run of the stress-strain curves registered dur-

ing mechanical loading of T300 composite denoted the absence of early cracks and general resistance to crack initiation and growth in this material. The result was that T300 carbon fibre composite was able to withstand the remarkable greater stress than the composite made of GRANOC. However it was stated earlier that GRANOC fibers had more ordered internal structure than T300 due to different fabrication process and different precursor, it should be mentioned that the first material suffers from relatively low inter-planar shear modulus what resulted in lower mechanical strength at high stress.

The microscopic inspection of T300 fibers had proven its more regular and more dense packaging within the filaments than that observed in the case of GRANOC fibers. The more regular packing of T300 fibers than GRANOC fibers and more uniform and dense micro-composition of that first composite is presented in Figures 2 and 3. In authors' opinion the T300 carbon fibre is a promising material that could be further used as the reinforcement in magnesium and magnesium alloy based composites. The possible applications of investigated Mg/C composites are primary military ones, as it was signaled in [13] but also lightweight vehicle and aircraft industries as well as a variety of prostheses for disabled persons.

Acknowledgement

Grant Agency of the Slovak Republic VEGA is acknowledged for supporting this work (Project No 2/0117/20).

REFERENCES

- [1] M. Gupta, W.L.E. Wong, *Mat. Charact.* **105**, 30-46 (2015).
- [2] A. Pawełek, A. Piątkowski, W. Wajda, W. Skuza, A. Tarasek, Z. Ranachowski, P. Ranachowski, W. Ozgowiec, S. Kúdela JR, S. Kúdela, *Arch. Metall. Mater.* **61**, 897-904 (2016).
- [3] J. Kuśnierz, A. Pawełek, Z. Ranachowski, A. Piątkowski, Z. Jasiński, S. Kúdela, S. Kúdela JR, *Rev. Adv. Mater. Sci.* **18**, 583-589 (2008).
- [4] M. Hagshenas, M. Gupta, *Def. Technol.* **15**, 123-131 (2019).
- [5] R. Islam, M., Hagshenas, *J. Magnes. Alloy.* **7**, 203-217 (2019).
- [6] Z. Xia, L. Xiaoxia, C. Shaokang, F. Yafu, *Int. J. Impact Eng.* **131**, 282-290 (2019).
- [7] Kúdela JR, H. Wendrock, S. Kúdela, A. Pawełek, A. Piątkowski, K. Wetzig, *Int. J. of Mat. Res.* **100**, 910-914 (2009).
- [8] S. Kúdela JR, P. Švec, O. Bajana, L. Orovčík, P. Ranachowski, Z. Ranachowski, *Kovove Mater.* **55**, 195-203 (2017).
- [9] N. Beronska, K. Iždinsky, P. Štefanik, S. Kudela, T. Dvorak, F. Šimančík, Z. Hajovska, A. Rusnak, *Kovove Mater.* **53**, 451-458 (2015).
- [10] H. Fukuda, K. Kondoh, J. Umeda, B. Fugetsu, *Mat. Chem. Phys.* **127**, 451-458 (2011).
- [11] A.A. Luo, *J. Magnes. Alloy.* **1**, 2-22 (2013).
- [12] O. Faruk, J. Tjong, M Sain (Ed.), *Lightweight and Sustainable Materials for Automotive Applications*, CRC Press, New York (2017).
- [13] <https://register.epo.org/application?number=EP16180665&tab=main>.
- [14] S.H. Han, H.J. Oh, S.S. Kim, *Compos. Sci. Technol.* **19**, 55-62 (2014).
- [15] M.R. Satapathy, B.G. Vinayak, K. Jayaprakash, N.K. Naik, *Mater. Des.* **51**, 347-356 (2013).
- [16] E.G. Sherwood, K.A. Soudki, *Compos. B – Eng.* **31**, 6-7 (2000).
- [17] M. Song, G.Wu, W.Yang, W.Jia, Z. Xiu, G.Chen *J. Mater. Sci. Technol.* **26**, 931-935 (2010).
- [18] H.Z. Ye, X.Y. Liu, *J. Mater. Sci.* **39**, 6153-6171 (2004).
- [19] A. Feldhoff, E. Pippel, J. Woltersdorf, *Adv. Eng. Mater.* **2**, 471-480 (2000).
- [20] S. Zhang, G. Chen, R. Pei, M. Hussain, Y. Wang, D. Li, P. Wang, G. Wu, *Mater. Des.* **65**, 567-574 (2015).
- [21] V.M. Karbhari, H. Strassler, *Dent. Mater.* **23**, 960-968 (2007).
- [22] M.V. Rao, P. Mahajan, R.K. Mittal, *Compos. Struct.* **83**, 131-142 (2008).
- [23] Y. Zeng, X. Xiong, G. Li, Z. Chen, W. Sun, D. Wang, Y. Wang, *Carbon*, **63**, 92-100 (2013).
- [24] https://www.ngfworld.com/dcms_media/other/Granocchopped2016.pdf
- [25] X. Zhou, X. Liu, S. Cui, Y. Fan, *Int. J. of Impact Eng.* **131**, 282-290 (2019).
- [26] H.G. Chae, B. Newcomb, P. Golgunje, Y. Liu, K. Gupta, M. Kar-math, K. Lyons, S. Ghosal, C. Pramanik, L. Gianuzzi, K. Sahin, I. Chasiotis, S. Kumar, *Carbon*, **93**, 81-87 (2015).